

Abstract

The effect of polar sea ice melt on low latitude climate is little known. In order to understand the response of Indian summer monsoon (ISM) to the sea ice melt, we have run a suite of coupled and uncoupled climate model simulations. In one set of simulations, the albedo of sea ice is changed in such a way that it would melt as a result of increased absorption of solar radiation. We find a substantial weakening of ISM in sea ice melt experiments. Further, the genesis frequency of monsoon low-pressure systems (LPS) declines by about 40% in the sea ice melt simulations. A weakening and equatorward shift of ITCZ causes the decline in LPS genesis. Overall, the response of ISM to the sea ice melt resembles the response to greenhouse gas induced warming.

Plain Language Summary

The Arctic and Antarctic sea ice are melting rapidly which can have feedback effects on climate system. However, the effect of sea ice melt on low latitude climate is not adequately understood. The Indian summer monsoon, known as the lifeline of Southeast Asia, is important to the water security of more than 1.5 billion people. We examined the response of Indian summer monsoon to the polar sea ice melt using a suite of global climate model experiments. Our simulations show that the monsoon circulation and rainfall weakens substantially in response to the sea ice melt. Further, the propagating precipitating vortices embedded in the monsoon circulation declined by about 40% in the sea ice melt experiments. Our results suggest that the Arctic and Antarctic sea ice melt can have serious implications on the water security of Southeast Asia.

1 Introduction

The effect of Arctic and Antarctic sea ice melt on tropical climate is little known until recently. However, the recent evidences suggest that the polar sea ice melt can affect the deep tropics. The sea ice melt can have far reaching effects on global climate system through surface energy imbalance and the response of ocean dynamics (Screen & Simmonds, 2010; Serreze & Barry, 2011). Due to the thermal inertia of the oceans, the effect of sea ice melt can persist for multiple seasons (Francis et al., 2009). Experiments using atmospheric general circulation models (AGCM) have shown that the Arctic sea ice depletion explains most of the seasonal pattern of high latitude climate response to enhanced green house gas (GHG) warming (Deser et al., 2010).

The effects of sea ice melt and the Arctic amplification on mid-latitude climate are clear through the changes in storm tracks, jetstream, and the Rossby wave activity (Rinke et al., 2017; Francis & Vavrus, 2012). These changes cause an increased frequency of extreme weather events, such as floods, heatwaves, and severe cyclonic storms in the mid and high latitude regions (Cohen et al., 2014; Budikova, 2009). The effects of sea ice melt on low latitude weather have only recently started receiving attention from the research community. One possible channel for the changes in the Arctic to influence the tropics is through the response of oceanic heat transport (Tomas et al., 2016). It is well known that the Atlantic meridional overturning cell, which plays a key role in oceanic heat transport, would weaken in response the Arctic sea ice melt (Sevellec et al., 2017; Liu & Fedorov, 2019). The effect of Arctic amplification on the atmospheric thickness and subsequent changes in the equatorward Rossby wave propagation can be another channel for Arctic to tropics teleconnection (Francis & Vavrus, 2012). However, the low latitude impact of the Arctic sea ice melt was not clear in terms of response of the extreme weather events (Barnes et al., 2014; Wallace et al., 2014). Possible teleconnection between the Arctic sea ice variability and the Asian summer monsoon has been suggested on intraseasonal scales (Guo et al., 2014; Krishnamurti et al., 2015; Chatterjee et al., 2021).

In climate model simulations, in the absence of ocean dynamics, the effect of Arctic sea ice melt is largely confined to regions poleward of 30°N while the addition of ocean dynamics resulted in an equatorward shift of the inter-tropical convergence zone (ITCZ) (Deser et al., 2015; Liu & Fedorov, 2019). When only the thermodynamic coupling is retained by suppressing dynamic coupling, the ITCZ and Hadley cell shifted poleward in response to the Arctic sea ice melt (Tomas et al., 2016). The changes in the mean position of ITCZ can affect the tropical cyclone (TC) genesis (Molinari & Vollaro, 2013; Berry & Reeder, 2014). Aquaplanet simulations suggest that poleward shift in ITCZ would result in an increased frequency of TC like synoptic scale weather systems (Ballinger et al., 2015). Deng et al. (2018) argued that the variability in the Arctic sea ice might influence the mid-Pacific trough which in turn can affect the TC genesis over the Northwest Pacific. The response of ocean dynamics to the sea ice melt can induce a global oceanic response (Deser et al., 2010; Liu & Fedorov, 2019). Such an oceanic response can have far reaching effects on earth’s climate system, including tropical cyclones and monsoons.

One of the reasons for a lack of understanding of the effect of sea ice melt on the genesis of high impact tropical weather systems is that the coarse-resolution simulations using coupled models do not resolve TCs and monsoon low-pressure systems (LPS). One way to overcome this issue is to run high-resolution AGCM simulations forced with the sea surface temperatures (SST) and sea ice concentrations (SIC) from coupled model experiments (Murakami et al., 2011; Sandeep et al., 2018). The effect of global sea ice melt on mean and synoptic scale features of ISM is not understood. The synoptic scale vortices embedded in the monsoon circulation, known as LPS, contribute more than half of the total precipitation over the continental India (Praveen et al., 2015; Hunt et al., 2016). Here we investigate the response of monsoon LPS to the global sea ice melt using a series of coarse-resolution coupled and high-resolution uncoupled climate model simulations.

2 Data and methods

A control experiment (CTRL) is performed by running the community earth system model (CESM) version 1.2.2 (Hurrell et al., 2013) in a fully coupled mode, with pre-industrial (B1850_CAM5) forcing, for 350 years. The atmosphere and land are configured with a 0.9x1.25 degree horizontal resolution while the ocean and sea ice share a variable resolution gx1v6 displaced pole grid. In another experiment, the CESM model is restarted from the 300th year of CTRL experiment and run for 50 years. In the latter experiment, we decreased the albedo of bare and ponded sea ice and snow cover on ice over the Arctic and Antarctic Oceans in the sea ice component of CESM. Specifically, we changed the parameters R_{ice} and R_{pnd} from 0 to -2. Also, we reduced the single scattering albedo of snow by 10% for all spectral bands. These settings are similar to Liu and Fedorov (2019). The changes in albedo will result in the melting of sea ice due to an increased absorption of solar radiation. We designate this simulation as sea ice melt experiment (SIME).

TCs and monsoon LPS are not adequately resolved in the coarse resolution coupled model simulations. In order to save computational resources, we have designed a set of high-resolution AGCM simulations using the community atmospheric model (CAM5). The CAM5 model is run at 50 km horizontal resolution and forced with the annual cycles of sea surface temperatures (SST) and sea ice concentrations (SIC) from the CTRL and SIME simulations. The annual cycles of monthly climatology of SST and SIC are constructed using the last 10 years of the CTRL and SIME simulations. The other forcing of CAM5 are fixed at year 2000 conditions for both the experiments. An ensemble of four runs of CAM5 have been done by slightly perturbing the SST boundary condition for both the experiments. Each annual cycle experiment span four years and first year is discarded in the analysis to avoid spin up. Similar high-resolution AGCM experiments forced with SST and SIC annual cycles from coupled models have been done by

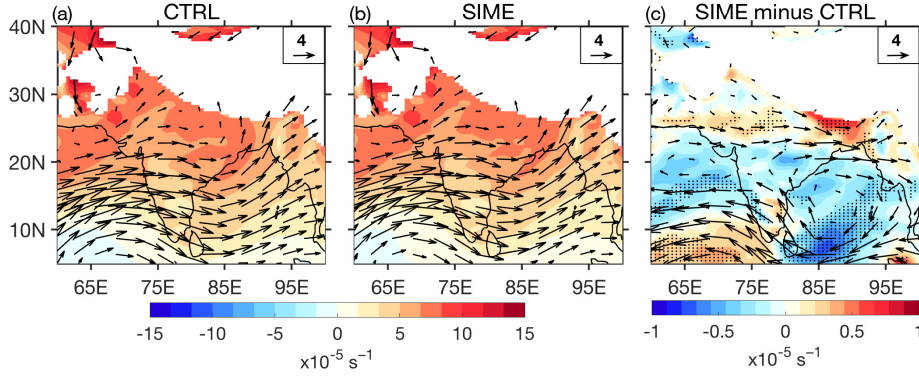


Figure 1. JJAS mean, ensemble mean wind vectors and absolute vorticity at 850 hPa for (a) CTRL and (b) SIME simulations, and (c) ensemble mean SIME minus CTRL wind vectors and absolute vorticity at 850 hPa. Stippling in (c) denote the statistically significant (at 95% confidence level) difference between SIME and CTRL absolute vorticity, as revealed by a t -test

114 Sandeep et al. (2018) to investigate the changes in LPS activity in a warming scenario.
 115 The results presented here pertain to the CAM5 ensemble mean, unless otherwise men-
 116 tioned.

117 The trajectories of LPS in the CAM5 simulations are tracked using Praveen et al.
 118 (2015) tracking algorithm. This algorithm detects and track LPS from gridded daily sea
 119 level pressure (SLP) data by identifying closed isobars at every 1 hPa interval. This al-
 120 gorithm also classifies the LPS according to their intensity category based on the pres-
 121 sure depth (Δ SLP). The categorization of monsoon LPS over the Indian region is shown
 122 in Table S1. Further, we have used the LPS data extracted by Praveen et al. (2015) from
 123 the daily gridded SLP of European Centre Interim Reanalysis (ERA-Interim). This data is also
 124 reported by Meera et al. (2019).

125 3 Results and Discussion

126 The ensemble mean June - September (JJAS) mean wind vectors and the absolute
 127 vorticity at 850 hPa resemble the typical Indian summer monsoon (ISM) low-level flow
 128 pattern (Fig. 1 a). The maximum low-level vorticity is seen over the monsoon trough
 129 region, extending from northwest India to the head Bay of Bengal. The head Bay of Ben-
 130 gal is the core genesis region of monsoon LPS (Sikka, 1977). The wind vectors and ab-
 131 solute vorticity climatology from SIME simulations also show a similar pattern as in the
 132 CTRL runs (Fig. 1b). In order to understand the difference between the two experiments,
 133 the difference in the wind vectors and absolute vorticity climatology between the two ex-
 134 periments is computed (Fig. 1c). The difference plot shows a weakening of low-level cir-
 135 culation and the absolute vorticity over the Indian region, with the maximum weaken-
 136 ing seen over the Bay of Bengal. These results suggest that the ISM circulation would
 137 weaken in response to the melting of the Arctic and Antarctic sea ice. Recent studies
 138 suggest that the polar sea ice melt in climate model simulations produces climate sys-
 139 tem response patterns reminiscent of global warming induced by greenhouse gas emis-
 140 sions (Liu & Fedorov, 2019; England et al., 2020). The annual climatology and seasonal
 141 cycle of the SIC from coupled model simulations show a substantial melting of the sea
 142 ice in both polar regions in SIME experiment (Fig. S1, S2). The SST climatology shows
 143 a warming over the tropical oceans (Fig. S3). It is interesting to note that the pattern
 144 of decline in SIC closely resembles that in the end of 21st century projections under RCP8.5
 145 scenario (Fig. S2). The ISM is known to weaken in a warming scenario and hence the

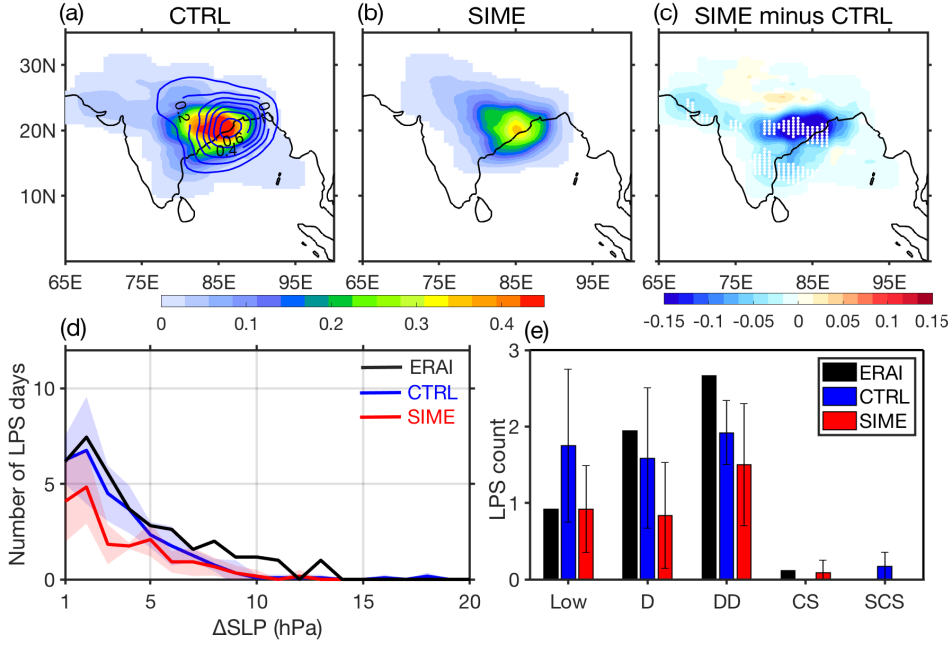


Figure 2. JJAS mean, ensemble mean LPS track density (unit: number of LPS per grid per season) for (a) CTRL and (b) SIME simulations; (c) ensemble mean difference between SIME and CTRL track density, (d) JJAS mean distributions of LPS days as a function of pressure depth (Δ SLP) of LPS, and (e) category-wise distribution of JJAS mean LPS counts in observations and model simulations. Stippling in (c) denote the statistically significant ($p < 0.05$) difference between SIME and CTRL LPS track density, as revealed by a t -test. The blue (red) shading in (d) shows the ensemble spread in CTRL (SIME) experiments. The error bars in (e) also show ensemble spread (± 1 *std*) in CTRL and SIME runs. The calculations using ERAI are done for the period 1979-2014.

146 weakening seen in response to the global sea ice melt is not entirely surprising (Krishnan
 147 et al., 2013).

148 Ditchek et al. (2016) found a relationship between the monthly mean fields of monsoon
 149 and the monthly LPS genesis. A weakening in the mean low-level circulation and
 150 the associated vorticity in a warming climate was attributed to a significant decrease in
 151 the monsoon LPS activity simulated by an AGCM (Sandeep et al., 2018). In this wake,
 152 we explore the changes in LPS activity over India in response to the polar sea ice melt.
 153 The ensemble mean track density of LPS in CTRL runs of CAM5 shows a maximum in
 154 the LPS genesis over the head Bay of Bengal and the adjoining continental India (Fig.
 155 2a). Further, the climatological LPS track density pattern in CTRL ensemble has a close
 156 match with the observations and the earlier high-resolution AGCM simulations (Krishnamurthy
 157 & Ajayamohan, 2010; Hurley & Boos, 2015; Sandeep et al., 2018; Thomas et al., 2021).
 158 The LPS track density shows about 32% weakening in the SIME ensembles in compar-
 159 ison to the CTRL runs (Fig. 2b). The difference plot between the CTRL and SIME track
 160 density shows a significant decrease in the LPS track density over the entire monsoon
 161 domain in the latter experiment. The weakening of LPS activity in response to the pol-
 162 ar sea ice melt is closely comparable to that in global warming projections, except for
 163 a lack of northward shift in the storm genesis (Sandeep et al., 2018). The poleward shift
 164 in the low-level monsoon circulation and the LPS genesis in global warming simulations

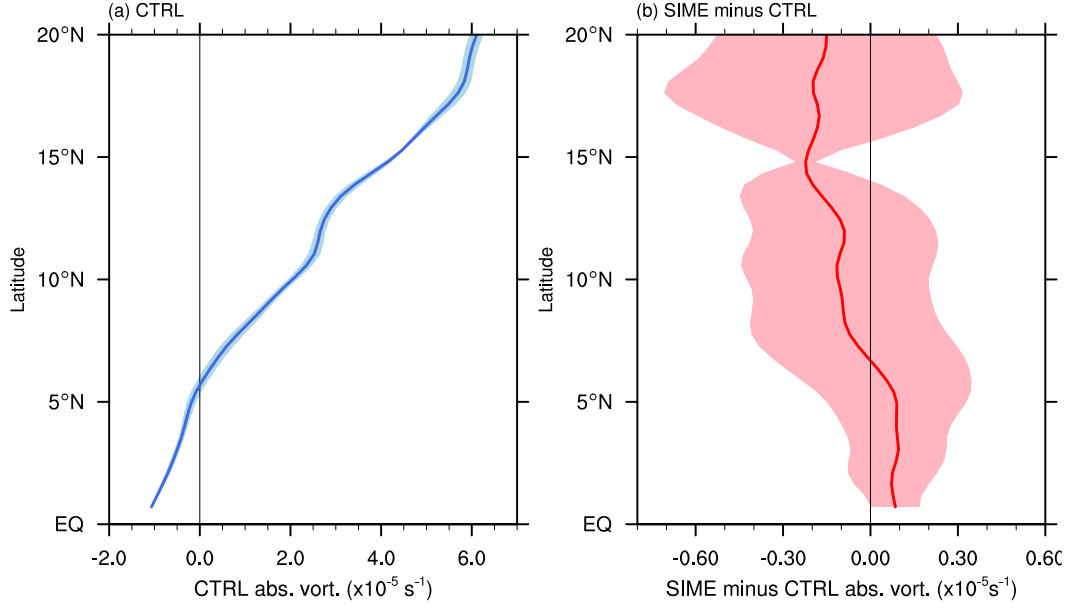


Figure 3. July-August mean zonal mean (50°E - 100°E) absolute vorticity at 850 hPa from (a) CTRL simulations and (b) difference in July - August mean absolute vorticity between SIME and CTRL simulations. The solid line shows ensemble mean and the shading ensemble spread

165 might be caused by an increase in the land-ocean temperature contrast over the South-
 166 east Asian region (Sandeep & Ajayamohan, 2015).

167 The decline in the LPS activity can be due to a decrease in the intensity of the storms
 168 or a decrease in the storm genesis frequency or a combination of the two. The distribu-
 169 tion of Δ SLP of LPS indicate the intensity of the storms during their life cycle (Fig. 2d).
 170 The model simulates the observed distribution of Δ SLP during the lifecycle of the storms,
 171 except for less number of high intensity storm days. The distribution of JJAS mean LPS
 172 counts in each intensity category shows that the CTRL ensembles have simulated more
 173 number of weaker LPS and less number of stronger LPS compared to the observations
 174 (Fig. 2e). Also, the SIME simulations show a decrease in the LPS numbers in all inten-
 175 sity categories, with about 40% decline across all categories. This suggest that the de-
 176 cline in the LPS activity is due to a decrease in the number as well as intensity of storms
 177 in the sea ice melt experiments.

178 Recent evidences suggest an equatorward shift in the ITCZ in response to the Arc-
 179 tic sea ice melt (Deser et al., 2015; Liu & Fedorov, 2019). Such a shift in ITCZ can re-
 180 sult in a weakening of the cyclogenesis (Merlis et al., 2013; Ballinger et al., 2015). We
 181 examine the changes in the regional ITCZ over the Indian monsoon region that may ex-
 182 plain the decline in LPS activity. The ITCZ can be identified as the centroid of max-
 183 imum precipitation or the latitude of low-level zero absolute vorticity (Tomas & Web-
 184 ster, 1997; Liu & Fedorov, 2019). The zonal mean ensemble mean July-August absolute
 185 vorticity at 850 hPa from the CTRL experiments show a change of sign at around 6°N
 186 and a maximum around 20°N (Fig. 3a). We choose July-August as it is the peak LPS
 187 genesis period. The ensemble mean difference in the July-August zonal mean absolute
 188 vorticity shows a weakening north of about 7°N and a relative strengthening in the equa-
 189 torward region (Fig. 3b). This is an indication of a decrease in the convergence over the
 190 core LPS genesis region and an equatorward shift in the ITCZ. A similar analysis us-
 191 ing zonal mean July-August precipitation over the region shows consistent result. One
 192 difference in the zonal mean profile of the precipitation is the presence of a bimodal peak,

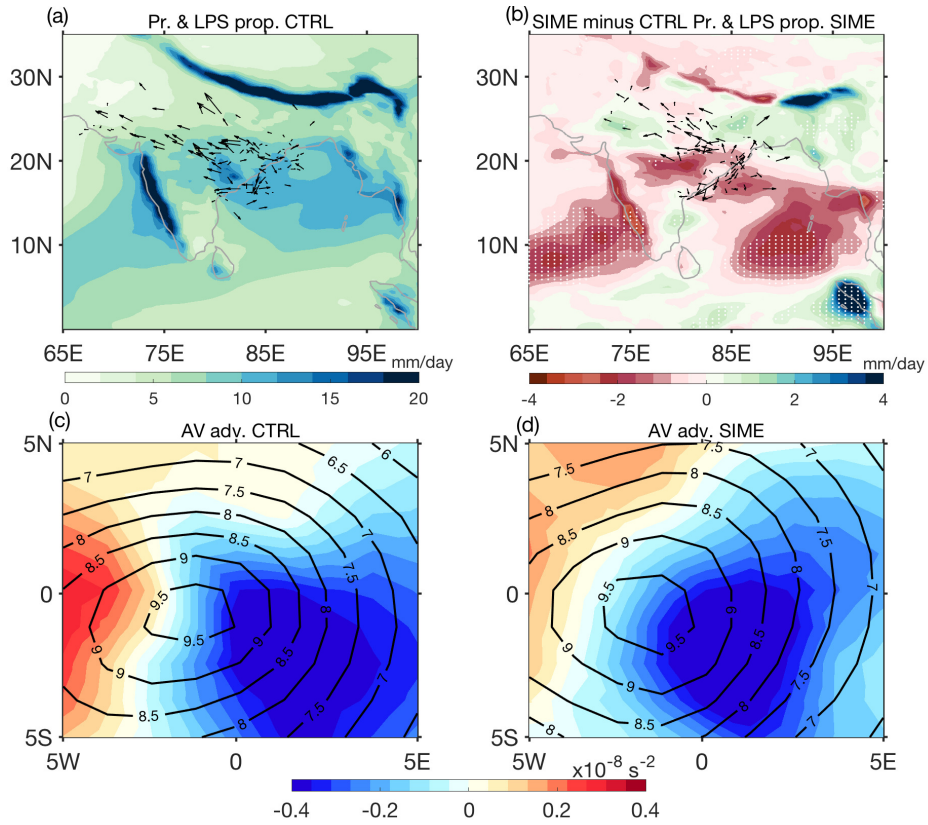


Figure 4. Top panel: (a) Ensemble mean JJAS mean precipitation (shading) LPS propagation vectors from CTRL and (b) difference in precipitation (shading) between SIME and CTRL, and LPS propagation vectors in SIME. Stippling shows statistically significant (at 95% confidence level) change in precipitation as revealed by a *t*-test. Bottom panel: Storm centered composites of 500 - 250 hPa averaged absolute vorticity (contours; units: $\times 10^{-5} \text{ s}^{-1}$) and absolute vorticity advection (shading; units: $\times 10^{-8} \text{ s}^{-2}$) for (c) CTRL and (d) SIME simulations.

193 with one between equator and 5°N and a larger peak around 18°N (Fig. S4). The dif-
194 ference in the zonal mean precipitation between SIME and CTRL shows a weakening
195 (strengthening) north (south) of 5°N, consistent with the changes in absolute vorticity.

196 The propagation of LPS to the deep interior parts of the Indian landmass plays a
197 crucial role in the distribution of precipitation during summer monsoon season. The en-
198 semble mean propagation vectors of LPS from the CTRL simulations show a north-westward
199 propagation (Fig. 4a) that is closely comparable with the observed horizontal advection
200 of LPS (Krishnamurthy & Ajayamohan, 2010; Hurley & Boos, 2015; Srujan et al., 2021).
201 The LPS propagation in SIME ensemble is weak and not penetrating to the northwest-
202 ern India (Fig. 4b). The seasonal mean precipitation climatology in CTRL ensemble shows
203 a band of non-orographic precipitation maxima aligned with the LPS propagation vec-
204 tors. A widespread weakening of ISM precipitation can be seen in SIME ensemble, a part
205 of which might be contributed by the weaker LPS activity. One of the suggested mech-
206 anisms of the LPS propagation is vorticity advection. The storm-centered composite of
207 500 - 250 hPa averaged absolute vorticity shows a maximum in the southwest quadrant
208 of the storm in the CTRL ensemble (Fig. 4c) as observed (Sikka, 1977; Hurley & Boos,
209 2015). The advection of absolute vorticity shows a westward propagation that explains
210 to a larger extent the simulated LPS propagation. In the SIME ensemble, the absolute
211 vorticity and the advection of the absolute vorticity associated with the simulated LPS
212 weaken (Fig. 4d). This explains the weaker LPS propagation in the SIME simulations.

213 4 Conclusions

214 The Arctic and Antarctic sea ice are projected to have ice free summers towards
215 the end of the 21st century in simulations of high emission scenarios. The global sea ice
216 melting is shown to affect tropical climate, primarily through ocean dynamics. However,
217 the effect of sea ice melt on major tropical climate systems such as Indian summer mon-
218 soon is not understood. We have performed a suite of coupled and uncoupled climate
219 model simulations to understand the impact of global sea ice melt on the Indian sum-
220 mer monsoon. Our results show that the ISM circulation would weaken significantly in
221 response to the global sea ice melt. Further, the monsoon LPS that are responsible for
222 more than half of the continental Indian rainfall weakens in the sea ice melt simulations.
223 The weakening and an equatorward shift of the ITCZ over the Indian monsoon region
224 cause a reduction in the LPS activity over the Bay of Bengal in the sea ice melt scenario.
225 Our analysis show that about 40% decrease in the number of LPS occurs in response to
226 the global sea ice melt. The horizontal advection of LPS also weakens in the sea ice melt
227 simulations. These results suggest that the polar sea ice melt can have a substantial im-
228 pact on the Indian summer monsoon through a weakening of the synoptic activity that
229 is crucial for rainfall distribution over land.

230 Acknowledgments

231 SS acknowledges funding support by the National Centre for Polar and Ocean Research,
232 Ministry of Earth Sciences, Government of India (NCPOR/2019/PACER-POP/OS-04).
233 The coupled and uncoupled simulations of CESM are performed on the HPC resources
234 of IIT Delhi.

235 Open Research

236 The CESM-CAM5 model simulations and LPS tracks data (Chandra, 2021) can
237 be accessed from <https://osf.io/bhqgd>.

238

References

- 239 Ballinger, A. P., Merlis, T. M., Held, I. M., & Zhao, M. (2015). The sensitivity
240 of tropical cyclone activity to off-equatorial thermal forcing in aquaplanet
241 simulations. *Journal of the Atmospheric Sciences*, *72*(6), 2286-2302. doi:
242 10.1175/JAS-D-14-0284.1
- 243 Barnes, E. A., Dunn-Sigouin, E., Masato, G., & Woollings, T. (2014). Exploring
244 recent trends in northern hemisphere blocking. *Geophysical Research Letters*,
245 *41*(2), 638-644. doi: 10.1002/2013GL058745
- 246 Berry, G., & Reeder, M. J. (2014). Objective identification of the intertropical con-
247 vergence zone: Climatology and trends from the era-interim. *Journal of Cli-*
248 *mate*, *27*(5), 1894 - 1909. doi: 10.1175/JCLI-D-13-00339.1
- 249 Budikova, D. (2009). Role of arctic sea ice in global atmospheric circulation: A re-
250 view. *Global and Planetary Change*, *68*(3), 149 - 163. doi: 10.1016/j.gloplacha
251 .2009.04.001
- 252 Chandra, V. (2021). *Substantial weakening of indian summer monsoon synoptic*
253 *activity in response to polar sea ice melt*. Retrieved from [https://osf.io/](https://osf.io/bhqgd)
254 [bhqgd](https://osf.io/bhqgd)
- 255 Chatterjee, S., Ravichandran, M., Murukesh, N., Raj, R. P., & Johannessen,
256 O. M. (2021). A possible relation between arctic sea ice and late season
257 indian summer monsoon rainfall extremes. *npj Clim Atmos Sci*, *4*. doi:
258 10.1038/s41612-021-00191-w
- 259 Cohen, J., Screen, J., Furtado, J., Barlow, M., Whittleston, D., Coumou, D., ...
260 Jones, J. (2014). Recent Arctic amplification and extreme mid-latitude
261 weather. *Nature Geosci*, *7*, 627-637. doi: 10.1038/ngeo2234
- 262 Deng, K., Yang, S., Ting, M., Hu, C., & Lu, M. (2018). Variations of the mid-Pacific
263 trough and their relations to the Asian-Pacific-North American climate: Roles
264 of tropical sea surface temperature and Arctic sea ice. *Journal of Climate*,
265 *31*(6), 2233-2252. doi: 10.1175/JCLI-D-17-0064.1
- 266 Deser, C., Tomas, R., Alexander, M., & Lawrence, D. (2010). The seasonal atmo-
267 spheric response to projected Arctic sea ice loss in the late twenty-first century.
268 *Journal of Climate*, *23*(2), 333-351. doi: 10.1175/2009JCLI3053.1
- 269 Deser, C., Tomas, R. A., & Sun, L. (2015). The role of ocean-atmosphere coupling
270 in the zonal-mean atmospheric response to arctic sea ice loss. *Journal of Cli-*
271 *mate*, *28*(6), 2168-2186. doi: 10.1175/JCLI-D-14-00325.1
- 272 Ditchek, S. D., Boos, W. R., Camargo, S. J., & Tippett, M. K. (2016). A genesis in-
273 dex for monsoon disturbances. *Journal of Climate*, *29*(14), 5189 - 5203. doi:
274 10.1175/JCLI-D-15-0704.1
- 275 England, M., Polvani, L., Sun, L., & Deser, C. (2020). Tropical climate responses
276 to projected Arctic and Antarctic sea-ice loss. *Nature Geoscience*, *13*, 275-281.
277 doi: 10.1038/s41561-020-0546-9
- 278 Francis, J. A., Chan, W., Leathers, D. J., Miller, J. R., & Veron, D. E. (2009).
279 Winter northern hemisphere weather patterns remember summer Arc-
280 tic sea-ice extent. *Geophysical Research Letters*, *36*(7), L07503. doi:
281 10.1029/2009GL037274
- 282 Francis, J. A., & Vavrus, S. J. (2012). Evidence linking Arctic amplification to ex-
283 treme weather in mid-latitudes. *Geophysical Research Letters*, *39*(6). doi: 10
284 .1029/2012GL051000
- 285 Guo, D., Gao, Y., Bethke, I., Gong, D., Johannessen, O. M., & Wang, H. (2014).
286 Mechanism on how the spring arctic sea ice impacts the east asian summer
287 monsoon. *Theor Appl Climatol*, *115*, 107-119.
- 288 Hunt, K. M. R., Turner, A. G., & Parker, D. E. (2016). The spatiotemporal struc-
289 ture of precipitation in Indian monsoon depressions. *Quart. J. Roy. Meteor.*
290 *Soc.*, *142*, 3195-3210.
- 291 Hurley, J. V., & Boos, W. R. (2015). A global climatology of monsoon low-pressure
292 systems. *Quarterly Journal of the Royal Meteorological Society*, *141*(689),

- 1049-1064. doi: 10.1002/qj.2447
- 293 Hurrell, J. W., Holland, M. M., Gent, P. R., Ghan, S., Kay, J. E., Kushner, P. J.,
294 ... Marshall, S. (2013). The community earth system model: A framework for
295 collaborative research. *Bulletin of the American Meteorological Society*, *94*(9),
296 1339 - 1360. doi: 10.1175/BAMS-D-12-00121.1
- 297
298 Krishnamurthy, V., & Ajayamohan, R. S. (2010). Composite structure of monsoon
299 low pressure systems and its relation to indian rainfall. *Journal of Climate*,
300 *23*(16), 4285-4305. doi: 10.1175/2010JCLI2953.1
- 301 Krishnamurti, T. N., Krishnamurti, R., Das, S., Kumar, V., Jayakumar, A., & Si-
302 mon, A. (2015). A pathway connecting the monsoonal heating to the rapid
303 arctic ice melt. *Journal of the Atmospheric Sciences*, *72*(1), 5 - 34. doi:
304 10.1175/JAS-D-14-0004.1
- 305 Krishnan, R., Sabin, T. P., Ayantika, D. C., Kitoh, A., Sugi, M., Murakami,
306 H., ... Rajendran, K. (2013). Will the South Asian monsoon over-
307 turning circulation stabilize any further? *Clim Dyn*, *40*, 187–211. doi:
308 10.1007/s00382-012-1317-0
- 309 Liu, W., & Fedorov, A. V. (2019). Global impacts of arctic sea ice loss mediated by
310 the atlantic meridional overturning circulation. *Geophysical Research Letters*,
311 *46*(2), 944-952. doi: 10.1029/2018GL080602
- 312 Meera, M., Suhas, E., & Sandeep, S. (2019). Downstream and in situ: Two
313 perspectives on the initiation of monsoon low-pressure systems over the
314 bay of bengal. *Geophysical Research Letters*, *46*(21), 12303-12310. doi:
315 10.1029/2019GL084555
- 316 Merlis, T. M., Zhao, M., & Held, I. M. (2013). The sensitivity of hurricane
317 frequency to ITCZ changes and radiatively forced warming in aquaplanet
318 simulations. *Geophysical Research Letters*, *40*(15), 4109-4114. doi:
319 <https://doi.org/10.1002/grl.50680>
- 320 Molinari, J., & Vollaro, D. (2013). What percentage of western north pacific tropical
321 cyclones form within the monsoon trough? *Monthly Weather Review*, *141*(2),
322 499 - 505. doi: 10.1175/MWR-D-12-00165.1
- 323 Murakami, H., Wang, B., & Kitoh, A. (2011). Future change of western north pacific
324 typhoons: Projections by a 20-km-mesh global atmospheric model. *Journal of*
325 *Climate*, *24*(4), 1154 - 1169. doi: 10.1175/2010JCLI3723.1
- 326 Praveen, V., Sandeep, S., & Ajayamohan, R. S. (2015). On the relationship
327 between mean monsoon precipitation and low pressure systems in cli-
328 mate model simulations. *Journal of Climate*, *28*(13), 5305-5324. doi:
329 10.1175/JCLI-D-14-00415.1
- 330 Rinke, A., Maturilli, M., Graham, R. M., Matthes, H., Handorf, D., Cohen, L.,
331 ... Moore, J. C. (2017). Extreme cyclone events in the Arctic: Wintertime
332 variability and trends. *Environmental Research Letters*, *12*(9), 094006. doi:
333 10.1088/1748-9326/aa7def
- 334 Sandeep, S., & Ajayamohan, R. S. (2015). Poleward shift in indian summer mon-
335 soon low level jetstream under global warming. *Clim Dyn*, *45*, 337–351. doi:
336 10.1007/s00382-014-2261-y
- 337 Sandeep, S., Ajayamohan, R. S., Boos, W. R., Sabin, T. P., & Praveen, V. (2018).
338 Decline and poleward shift in indian summer monsoon synoptic activity in
339 a warming climate. *Proc. Natl. Acad. Sci. USA*, *115*(11), 2681–2686. doi:
340 10.1073/pnas.1709031115
- 341 Screen, J. A., & Simmonds, I. (2010). Increasing fall-winter energy loss from the
342 Arctic ocean and its role in Arctic temperature amplification. *Geophysical Re-*
343 *search Letters*, *37*(16). doi: 10.1029/2010GL044136
- 344 Serreze, M. C., & Barry, R. G. (2011). Processes and impacts of Arctic amplifica-
345 tion: A research synthesis. *Global and Planetary Change*, *77*(1), 85 - 96. doi:
346 10.1016/j.gloplacha.2011.03.004
- 347 Sevellec, F., Fedorov, A., & Liu, W. (2017). Arctic sea-ice decline weakens the At-

- 348 lantic meridional overturning circulation. *Nature Clim Change*, 7, 604–610.
349 doi: 10.1038/nclimate3353
- 350 Sikka, D. R. (1977). Some aspects of the life history, structure and movement of
351 monsoon depressions. *PAGEOPH*, 115, 1501–1529. doi: 10.1007/BF00874421
- 352 Srujan, K. S. S. S., Sandeep, S., & Suhas, E. (2021). Downstream and in situ genesis
353 of monsoon low-pressure systems in climate models. *Earth and Space Science*,
354 8(9), e2021EA001741. doi: <https://doi.org/10.1029/2021EA001741>
- 355 Thomas, T., Bala, G., & Srinivas, V. (2021). Characteristics of the monsoon low
356 pressure systems in the indian subcontinent and the associated extreme precip-
357 itation events. *Clim Dyn*, 56, 1859–1878. doi: 10.1007/s00382-020-05562-2
- 358 Tomas, R. A., Deser, C., & Sun, L. (2016). The role of ocean heat transport in the
359 global climate response to projected Arctic sea ice loss. *Journal of Climate*,
360 29(19), 6841–6859. doi: 10.1175/JCLI-D-15-0651.1
- 361 Tomas, R. A., & Webster, P. J. (1997). The role of inertial instability in determin-
362 ing the location and strength of near-equatorial convection. *Quarterly Journal*
363 *of the Royal Meteorological Society*, 123(542), 1445–1482. doi: [https://doi.org/](https://doi.org/10.1002/qj.49712354202)
364 [10.1002/qj.49712354202](https://doi.org/10.1002/qj.49712354202)
- 365 Wallace, J. M., Held, I. M., Thompson, D. W. J., Trenberth, K. E., & Walsh, J. E.
366 (2014). Global warming and winter weather. *Science*, 343(6172), 729–730. doi:
367 [10.1126/science.343.6172.729](https://doi.org/10.1126/science.343.6172.729)